LARGE SIGNAL CHARACTERIZATION AND NUMERICAL MODELING OF THE GaAs/AlGaAs HBT

Douglas A. Teeter, Student Member, IEEE, Jack R. East, Member, IEEE,
Richard K. Mains, Member, IEEE, George I. Haddad, Fellow, IEEE

Department of Electrical Engineering and Computer Science
University of Michigan, Ann Arbor, MI 48109-2122.

Abstract: A numerical model for GaAs/AlGaAs HBT's which includes velocity overshoot effects has been developed. Good agreement between measured and modeled small signal characteristics has been obtained. To understand the large signal performance of the HBT, the model has been used to parameterize several typical device structures. At low frequencies, the parametarization method describes the large signal behavior of the HBT reasonably well up to moderate power levels. At higher frequencies, the accuracy of the method degrades. High frequency simulation results have been compared with measurements made with a 26.5 to 40 GHz active load pull system. Details of the measurement system, sources of error, and methods to reduce the error are discussed. [1]

I. Introduction

The heterojunction bipolar transistor has proven itself to be a useful device for high frequency power applications [1]. In designing power circuits with any transistor, it is necessary to know the dependence of the device characteristics on RF drive level. The purpose of this work is to determine the large signal properties of the heterojunction bipolar transistor through numerical modeling and large signal measurements.

II. Model Formulation

The model simulates the active device by simultaneously solving the Poisson equation, continuity equations, and an electron energy equation in one dimension. The equations are similar to the formulation in [2]. Given time varying base and collector voltages, internal carrier concentrations, electric fields, and electron velocities are computed. From these quantities, the terminal currents are calculated. Small signal characterisicts of the device are computed by applying a small step voltage perturbation first to the input port and then to the output port. The terminal data from the perturbation is then Fourier analyzed to compute the small signal y parameters of the transistor. Parasitic elements, obtained from measurements of a transistor with the same device structure, are added using Touchstone©.

The simulation can also be used to study the large signal performance. Power dependent "Y" parameters can be found by applying a sinusiodal RF voltage of various amplitudes to the input port of the transistor with the output voltage fixed. The time varying device currents are used to calculate the device "Y" parameters as a function of input voltage amplitude. The same approach is taken to characterize the output port. This characterization of the active device is then embedded in a circuit which models device parasitics. Using these results, the power performance of the device can be predicted.

[1]This work is being supported by the Army Research Office under the URI program, Contract No. DAAL03-86-K-0007.

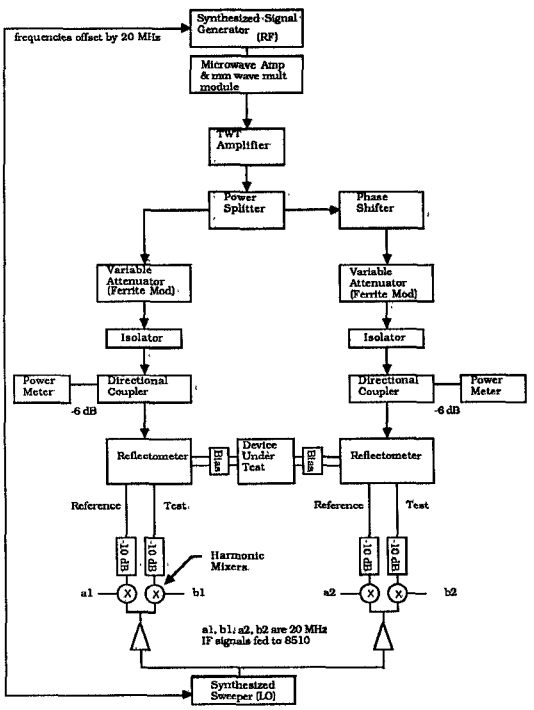

Fig. 1. Active Load Pull System

III. Measurement System

There are several techniques for large signal device measurement and characterization. Passive tuners are commonly used to measure load pull contours. However, at 26.5 to 40 GHz, the high insertion loss of the bias tees available in our lab made this approach impractical. To circumvent this problem, an active load pull measurement system has been constructed using the same principles found in [3] and [4]. Figure 1 depicts this system. By varying the magnitude and phase of the incident signal at port 2 with respect to the incident signal at port 1, one is able to electronically impose any load impedance on the DUT.

A complete error analysis of the measurement system has been performed. A major source of error in any load pull system is inaccuracy in the reflection coefficient measurement. At higher reflection factors, this error increases. This can be explained if one considers the equations used to compute input and load power:

$$P_{in} = P_{inc}(1 - |\Gamma_{in}|^2) \quad (1)$$

$$P_{load} = P_{out}(1 - |\Gamma_{load}|^2) \quad (2)$$

OF-II

For example, a worst case difference of 0.2 dB in Γ results in less than 0.01 dB error in calculated power for $\Gamma = 0.2$ but results in almost 1 dB error for $\Gamma = 0.9$. In order to calibrate out most of this error, a one tier extended TRL calibration is used. Total uncertainty in system calibration is less than 0.15 dB, resulting in a maximum error in computed power gain of about 1 dB for a reflection factor of 0.8. Approximately 0.6 dB of this error can be attributed to reflection uncertainty. The remaining portion of the error arises from uncertainty in the source match term used for input power correction and from power meter repeatability.

A critical factor for calibration accuracy in any measurement system is the quality of the signal path between the reflectometers and the DUT. The main limitation of our present system are our bias tees. While the bias tees are within manufacturer's specifications, the 11 dB return loss is not adequate for our application. Any small change in return loss of the bias tee between calibration and measurement results in serious errors. A simple computer simulation indicates that using bias tees with 16 dB return loss will greatly improve measurement accuracy.

A novel scheme of extracting the fixture S parameters has been developed. These parameters are used to compute the power levels at the terminals of the DUT. First, a TRL calibration of the test fixture is performed. This calibration is converted to two 1 port calibrations. With port 2 calibration on, a short, offset short, and a load are connected to the input half of the fixture and measured. From this data, a one port calibration is computed; the resulting error coefficients are the S parameters of the input half of the test fixture. To check this procedure, these S parameters are cascaded to a 1 port calibration at the input of the test fixture. This calibration is compared to the original TRL calibration for an offset short. The disagreement is less than 0.15 dB over most of the 26-40 GHz frequency band. Note that these fixture S parameters are used only in calculating power at the terminals of the DUT and not for reflection coefficient measurement.

IV. Results

Below are tables describing the AlGaAs/GaAs HBT device structures measured and modeled.

Measured Device [6]

region	Al frac	dop	dop (cm^{-3})	μm
contact	0.0	n	3.E18	0.1
emitter	0.3	n	5.E17	0.2
spacer	0.0	n	undoped	0.02
base	0.	p	5.E19	0.1
collector	0.	n	3.E16	0.5
sub collector	0.	n	3.E18	0.5

Structure I

region	Al frac	dop	dop (cm^{-3})	μm
contact	0.0	n	2.E18	0.08
grading	0-0.3	n	5.E17	0.03
emitter	0.3	n	5.E17	0.14
emitter grading	0.3-0.	n	5.E17	0.03
base	0.	p	2.E19	0.1
collector	0.	n	3.E16	0.5
sub collector	0.	n	2.E18	0.1

Structure II

region	Al frac	dop	dop (cm^{-3})	μm
contact	0.	n	2.E18	0.08
grading	0.-0.3	n	1.E18	0.03
emitter	0.3	n	3.E17	0.081
emitter grading	0.3-0.	n	3.E17	0.03
base	0.	p	1.E19	0.1
collector	0.	n	3.E16	1.5
sub collector	0.	n	2.E18	0.1

A. *Small Signal Results*

To verify the validity of our model, the small signal characteristics of structure I were computed. Figure 2 compares measured and calculated f_T. Our model assumes a constant lattice temperature of 300 K. While our simulations compare favorably to published Monte Carlo results for a constant lattice temperature [5], the measured data indicates that thermal effects become significant at high current densities. These thermal effects result in increased scattering rates which cause the leveling in measured f_T. Comparison between measured and modeled small signal parameters from 8 to 35 GHz are made in figures 3 and 4 for I_b =3.5 mA, V_{CE} =3 V, and I_c =9 mA. Considering the model is *purely physical, derived from first principles, and uses no fitting parameters,* the agreement is very good. Disagreement at lower frequencies increases because the measured device has abrupt heterojunctions while the simulated device uses graded heterojunctions. This difference manifests itself as a slightly different equivalent circuit for the two structures; the primary difference being that α_o used in the graded device equivalent circuit is much closer to 1. Changing α_o to 1 in the measured device equivalent circuit removed most of the disagreement at lower frequences. Because the purpose of our modeling is to better understand and explain our measured results, the additional effort required to include abrupt heterojunctions in the simulations is not necessary.

B. *Large Signal Results*

To examine the model at 10 GHz, structure II was used to simulate a 10 finger common emitter device published in the literature [7].

A calculated load pull power gain contour for this device at 10 GHz for $Z_S = 4.3 + j4.1\Omega$ (conjugate match) is given in

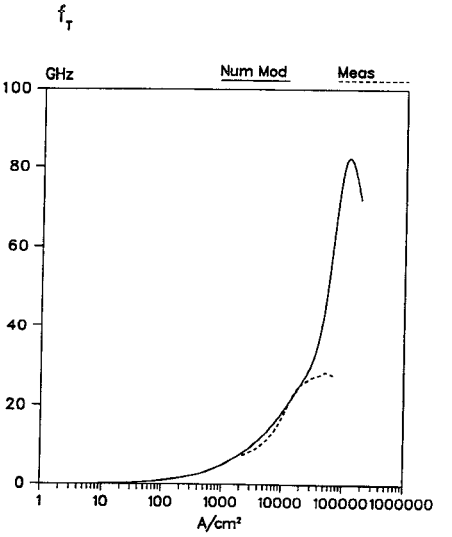

Fig. 2. f_T for V_{CE}=3 V

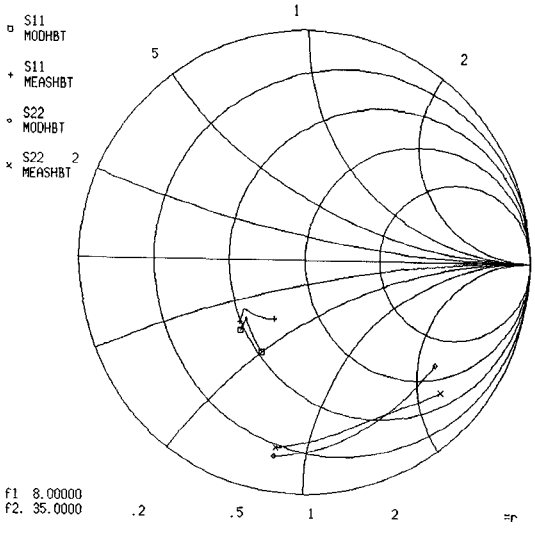

Fig. 3. S_{11} and S_{22}

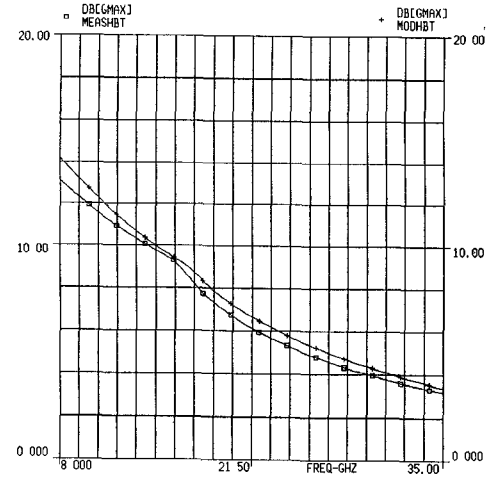

Fig. 4. Measured & Modeled G_{max}

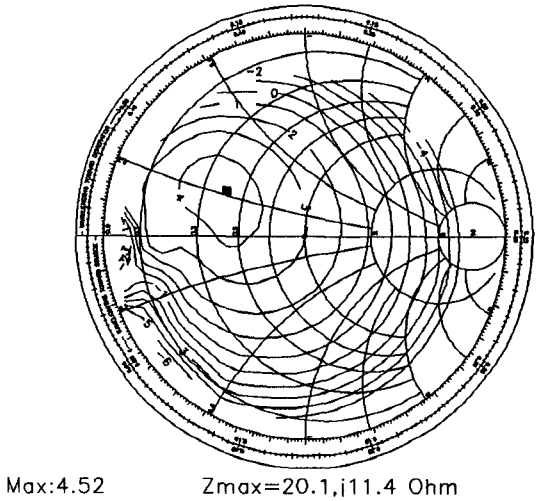

Fig. 5. Modeled G_P Circles P_{in} = 12 dBm

figure 5 (the transmission lines shown in [7] were omitted from our calculations). From the published small signal parameters, the optimum low power load for the given Z_S is $Z_L = 12.0 + j22.4\Omega$, close to our low power model prediction of $Z_L = 16.3 + j16.5\Omega$. The simulated low power available gain for the given Z_S was 5 dB, close to the 6 dB computed from the published S parameter data. Because a one dimensional model was used, the effective device area was estimated by computing the area needed to make the modeled collector base capacitance agree with the value extracted from the published equivalent circuit.

To characterize HBT's at 27 GHz, our active load pull system was used. Devices from various sources were measured. A typical result (I_b =3.5 mA, V_{CE} =3 V, and I_c =9 mA) for the measured structure given earlier is shown in figure 6 (this result includes the bond wires).

The graph in figure 7 compares measured and modeled power gain as a function of input power with a constant load impedance on the transistor (the load used is optimum for low power). Differences between the two measured results are caused by several factors. The most obvious reason is that the measurements are for two different devices which are nominally the same. Slight differences in the bond wires and the device processing, however, could cause some variation in measured gain. Another source of discrepancy is the system measurement technique and calibration. Since results shown were made with system calibrations performed on different days, some of the difference in the data could be due to the 1 dB uncertainty in the measurement.

In measurement 1, the base was biased with a constant voltage source while in measurement 2, the base was biased

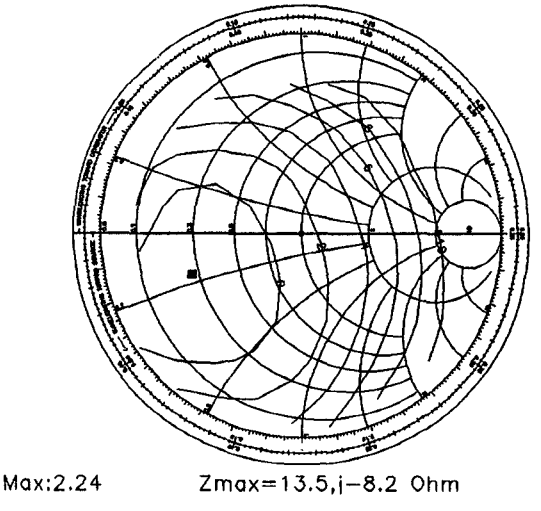

Fig. 6. 27 GHz G_P Circles for P_{in} = 17 dBm

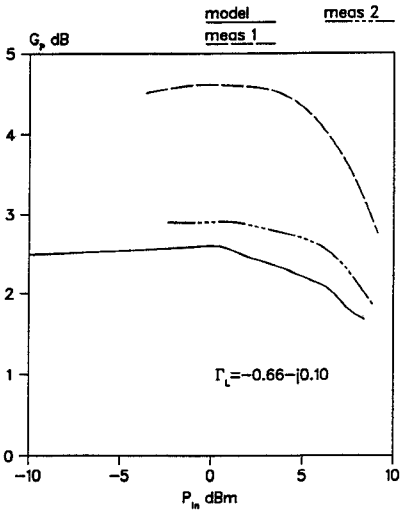

Fig. 7. 27 GHz G_P vs P_{in}

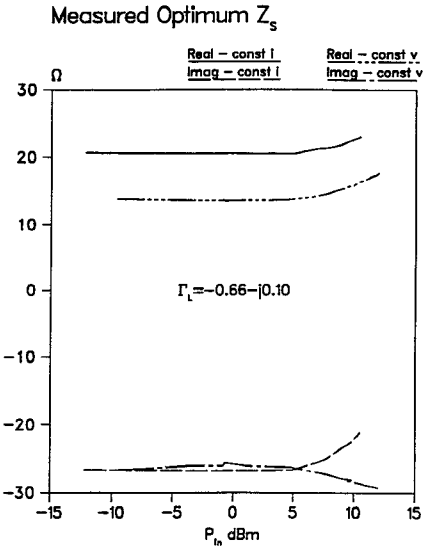

Fig. 8. 27 GHz Measured Z_S^{opt} vs P_{in}

with a constant current source. For the constant voltage source case, the base voltage was adjusted so that the DC base current with no RF drive was the same as the current source case. The trend predicted by the model agrees with the measured results. However, the model attributes most of the gain compression to a change in optimum load as the input power increases. Our measured data does indicate some shift in the optimum load as power is increased, but it is not nearly as pronounced as the model predicts.

In addition to measuring constant gain contours, the active load pull approach measures the input impedance of the device for each load. This data can then be used to find the optimum source impedance for a given frequency, load, and input power drive. Figure 8 shows the measured variation in real and imaginary optimum source impedance as input power increases (the load is kept at the low power optimum value). Since the measurements include the bond wires, the optimum reactance is capacitive.

V. Conclusion

A numerical model has been described. Agreement between the model and small signal measurements is excellent. To examine HBT operation under large signal conditions, drive level dependent "Y" parameters were used. At X-band, this approach qualitatively describes the large signal device behavior up to moderate power drive. At 27 GHz, our active load pull system was used to characterize an HBT under constant current and constant voltage base bias. Measured and modeled power gain at the optimum small signal load appear to agree. However, our preliminary results show that the model attributes much more of the gain compression to mismatch than indicated by our measurements.

VI. Acknowledgments

The authors would like to thank the following individuals for their helpful discussions and assistance: Phil Marsh, Marcel Tutt, Dave Pehlke and Jim Steimel. We would also like to thank Mike Adlerstein and Marco Afendykiw for providing us with HBTs to characterize. Load pull graphics software courtesy of Focus Microwaves, Inc.

References

[1] B Bayraktaroglu *et al.*, "5 W Monolithic HBT Amplifier for Broadband X-band Applications," *IEEE Microwave and Millimeter Wave Monolithic Circuits Symposium*, 1990, pp. 43-46.

[2] P. Sandborn, *et al.* "Quasi-Two-Dimensional Modeling of GaAs MESFET's," *IEEE Trans. Electron Devices*, May 1987, pp. 985-991.

[3] D. C. Yang & D. F. Peterson, "Large-Signal Characterization of Two-Port Nonlinear Active Networks," *IEEE MTT-S Digest*, 1982, pp. 345-347.

[4] R. Actis & R. A. McMorran, "Millimeter Load Pull Measurements," *Applied Microwave*, Nov/Dec 1989, pp. 91-102.

[5] Riichi Katoh & Mamoru Kurata, "Self-Consistent Particle Simulation for (AlGa)As/GaAs HBT's Under High Bias Conditions," *IEEE Trans Electron Devices*, October, 1989, pp. 2122-2128.

[6] Device provided by Raytheon Company, Research Division.

[7] B. Bayraktaroglu, *et al.* "2.5 W CW X-Band Heterojunction Bipolar Transistor," *IEEE MTT-S Digest*, 1989, pp. 1057-1060.